Applied Surface Science Advances 30 (2025) 100869

Contents lists available at ScienceDirect

Applied Surface Science Advances

journal homepage: www.sciencedirect.com/journal/applied-surface-science-advances

Full Length Article

Advanced IR polarimetry to study morphology and structure of ultrathin films

Karsten Hinrichs [a,*], Fatima Akhtar [a], Merve Buldu-Akturk [b], Andreas Furchner [a], Iver Lauermann [c], Norbert H. Nickel [a], Jörg Rappich [a]

[a] Nanoscale Solid–Liquid Interfaces, Helmholtz-Zentrum Berlin für Materialien und Energie, Schwarzschildstraße 8, Berlin 12489, Germany
[b] Helmholtz Young Investigator Group Electrocatalysis: Synthesis to Devices, Helmholtz-Zentrum Berlin für Materialien und Energie, 12489 Berlin, Germany
[c] Competence Centre Photovoltaics Berlin – PVcomB, Helmholtz-Zentrum Berlin für Materialien und Energie, Schwarzschildstraße 3, 12489 Berlin, Germany

ARTICLE INFO

Keywords:
Passivated interfaces
Functionalized interfaces
Infrared polarimetry
Degradation
Optical simulation
Interface structure

ABSTRACT

We demonstrate an infrared (IR) polarimetric approach for the detailed analysis of structural and morphological interface properties via the inspection of bands related to a pair of vibrations with perpendicular transition dipole moments. Performing polarization dependent IR spectroscopy and supplementary X-ray photoelectron spectroscopy (XPS) measurements, freshly prepared H/Si(111) surfaces as well as their long-term degradation in dry air environment and after exposure to humid air are investigated. Vibrational bands related to Si-H bending and Si-H stretching modes are discussed in conjunction with analytical optical simulations, elucidating the status of passivation and influence of varying domain sizes and oscillator densities. Notably, the vibration related to a strong out-of-plane directed transition dipole moment is extremely sensitive to the morphology and structure of the surface, whereas the in-plane directed band serves as a sensitive sensor for the overall status of the functionalization or passivation. Studies limited to only one of these bands may result in misleading conclusions on the passivation status, the pathway of degradation or structural properties. The analytic concept is also applied for the interpretation of vibrational bands of a methyl monolayer on Si(111). IR polarimetry is performed in a single reflection geometry which, compared to often used ATR geometries, is not restricted to specifically designed IR transparent substrates and also gives higher flexibility to potential adaptions to measurement chambers and cells. Our approach offers advanced possibilities for analysis in the field of interface science and contributes to a deeper understanding of interface properties. It is relevant for applications relying on specific interface properties, such as sensing, catalysis, photovoltaics, and electronics.

1. Introduction

Passivated surfaces are widely used in sensing and electronic applications. Often, it is required to understand the structural properties of the initial surface prior to further processing steps. In particular, the H-passivated Si(111) surface is assumed to be a surface with a high degree of perfection [1]. It can be prepared outside of ultra-high vacuum (UHV) conditions by wet-chemical processing [2–4]. Technologically, H-passivated Si(111) is a very interesting material for further chemical processing steps without the need of UHV environments. It can be utilized for effective molecular functionalization [5–7], sensing [7], electronic applications [7] as well as custom-sized nanopatterning [8], metal/silicon contacts [9–11] and in a-Si/c-Si solar cells [12–15].

The defect density of the best chemically prepared surfaces is expected to be lower than that of Si(111)-(1 $\times$ 1) prepared by H exposure under UHV conditions [16], but UHV preparations may be less contaminated [16]. However, an optimization of the preparation with respect to the reduction of defects and possible contaminations would be required to push the potential of H/Si(111) surfaces toward new applications, as is the case for Si(100) surfaces where individual atoms can be manipulated, e.g., for manufacturing of silicon electronics [17] and quantum devices [18].

When passivating a Si(111)-(1 $\times$ 1) surface, it is assumed that, at the end of the etching mechanism [19], hydrogen fully saturates the dangling bonds of the top layer's silicon atoms [19,20]. A multitude of experimental and theoretical studies have been performed for detailed investigations of the vibrational properties of this surface. The phonon dispersion throughout the surface Brillouin zone (SBZ) was calculated

* Corresponding author.
E-mail address: karsten.hinrichs@helmholtz-berlin.de (K. Hinrichs).

https://doi.org/10.1016/j.apsadv.2025.100869
Received 1 August 2025; Received in revised form 20 September 2025; Accepted 2 October 2025
Available online 10 October 2025

by density functional perturbation theory [20,21]. Localized optical phonon bands related to a Si-H in-phase stretching mode and a degenerated bending mode were found above the Si-bulk vibrational bands. It is well-established that these characteristic modes of H-passivated Si (111) surfaces can be sensitively studied by vibrational spectroscopies [1–3,22–31]. He-atom scattering (HAS) [22] and (HR)EELS [23,24] can reveal phonon dispersions throughout the surface Brillouin zone. However, a drawback of these techniques is often a limited spectral resolution. For measurements at high spectral resolutions, IR spectroscopy is the method of choice, although only measurements close to the Γ-point of the SBZ can be performed. Numerous IR spectroscopic investigations exist for bare and modified hydrogen passivated Si(111) surfaces [1–3,25–42]. Interestingly, due to the orientation of the Si-H bond perpendicular to the Si(111) surface, the stretching vibration exhibits only a transition dipole moment in direction of the surface normal and the bending vibration a transition dipole moment parallel to the surface [32] (Fig. 1a). Polarization dependent IR spectroscopy is advantageous for the investigation of such a characteristic behavior (Fig. 1b). In p-polarized and ellipsometric tanΨ spectra, the bands related to the in-plane and out-of-plane oriented vibrations typically point upward and downward, respectively. This characteristic behavior can be applied for a qualitative inspection of average orientations of bonds and molecules [43]. Orientation of the Si-H transition dipole moment normal to the surface plane facilitates conclusive studies of vibrational band properties such as frequency, amplitude and shape in p-polarized reflection spectra (or ellipsometric $\tan\Psi = \sqrt{R_p/R_s}$ spectra). It is of advantage for the analysis that the band shape is not disturbed by an overlapping contribution of the related in-plane vibrational absorption [44].

Comprehensive studies of H-passivated surfaces have been performed for decades [1–3,26–28]. The frequency, intensity and width of the band related to the Si-H stretching vibration for a freshly prepared H/Si(111) surface was found to be a marker for the quality of the prepared surface [2]. It was concluded that *"the more homogeneous the surface the narrower the absorption line and the higher the Si-H stretch frequency"* [2]. Band frequencies of 2083.92 cm^{-1} [2] and 2083.7 cm^{-1} [3] were measured for the initial passivated Si surface with ideally terminated (111) domains. For such surfaces, the number of defects is expected to be < 1 % of the monolayer (ML) [2,3]. In-situ scanning tunneling microscopy (STM) of H/Si(111) revealed the surface structure with atomic resolution, showing that flat passivated domains are not defect-free and also areas with no clear atomic structure may exist [4]. IR spectra may also be sensitive to imperfections, such as variations of the finite-sized (1 × 1) domains; other Si-H modes than in-phase may contribute to an anisotropic tail and band broadening [27]. Additional peaks are expected for Si-H attached to other Si-Si bonding arrangements [3], contributions of SiH_2 and SiH_3 modes [26,40] and defect modes [2]. In addition, strain can significantly change the Si-H stretching and bending related band intensities [29].

In our preparations of functionalized Si(111) surfaces [33–38], applied for electronic or sensing applications, we often used an H-passivated surface as the starting point for further processing, such as the termination by aryl groups [36–38] or methyl and ethynyl groups [34,35]. As discussed above, a well-known approach for a quality check of a freshly H-passivated surface is an IR spectroscopic analysis in the range of the Si-H stretching vibrations.

Using literature work as reference, it seems to be straightforward to qualitatively interpret the measured spectra of passivated Si(111) in this range, e.g., to identify in-phase Si-H stretching vibrations [2,3]. However, imperfect surfaces may show complex spectra depending on many factors, such as steps [26,40,42], steric interactions [39], strain [26], defects [2] and oxidation [31,41]. For example, the vibrational pattern of a vicinal or nanorough Si(111) surface in the Si-H stretching range shows a complex vibrational signature due to the overlay of different vibrational contributions [26,39,40]. A detailed assignment was recently revealed by a combined DFT and experimental study [39].

The frequency and half width of the band related to in-phase Si-H stretching vibrations might serve as an indicator for the quality of well-ordered Si(111) domains [2]. Therefore, seeing the sharp band related to the Si-H stretching vibration at the expected frequency of about 2083.8

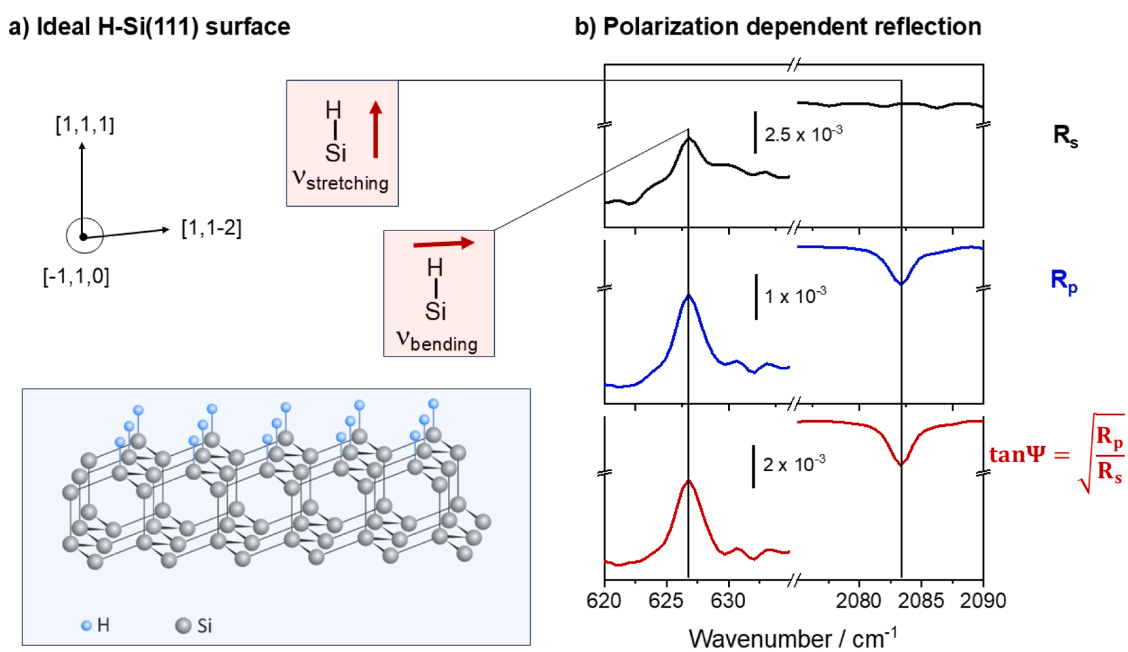

Fig 1. a) Sketch for an ideal Si(111)-H surface structure (Si represented by grey and H by blue spheres). The direction of transition dipole moments is indicated by red arrows. The Si-H stretching vibration is oriented perpendicular to the surface plane, whereas the one of the Si-H bending vibration is in-plane oriented. b) Polarization dependent reflection spectra. s-polarized reflection (R_s, spectrum, top) can only probe the bending vibration, as s-polarized radiation has only in-plane field components. p-polarized reflection (R_p, spectrum in the middle) can probe both the bending and the stretching vibration, as p-polarized radiation consists of both in-plane and out-of-plane field components. The same holds for the ellipsometric parameter tanΨ (bottom spectrum), which is calculated from the square root of the ratio of R_p and R_s.

cm^{-1} can be taken as a marker that the initial surface is of high quality. However, such a procedure focusing merely on the sharp Si-H stretching related band provides only a limited view on the passivation properties and may lead to misinterpretations about the quality of the passivation. For example, taking the absence of this Si-H stretching band as a sign that the surface is not passivated is a misleading conclusion.

Fig. 2 shows a typical p-polarization dependent reflection spectrum for an H-passivated Si(111) surface. The spectrum with a resolution of 0.5 cm^{-1} shows a band maximum close to 2084 cm^{-1} for the initially H-passivated surface. A band at 2083.84 ± 0.01 cm^{-1} with a width of Γ = 1.41 ± 0.03 cm^{-1} is determined by a Lorentz fit. In this respect, our results seem to correlate well with those found in literature [2,3]. Because the interpretations of spectra can be improved by optical modeling, we will discuss in the experimental part the following issues: How can amplitudes and frequencies of a vibrational band be qualitatively interpreted for the H-Si(111) surface and what conclusions can be drawn about the surface structure and morphology? Such discussions are relevant for a broader field of research on passivated and functionalized surfaces. As an example for a functionalized surface, the results section is completed by a discussion of IR polarimetric spectra of a CD_3 functionalized Si(111).

2. Methods

2.1. Sample preparation

H-passivation of the Si(111) surface was performed as follows: the Si sample (p-doped Si(111) ± 0.5°, 0.02–0.03 Ωcm from Siegert Wafer or University Wafer) was cleaned in an ultrasonic bath with isopropanol, rinsed with high-purity water and ozonized for 30 min. Afterwards it was etched for 4 min in 40 % NH_4F solution, rinsed again with high-purity water, and dried under nitrogen flow. Subsequently, the sample was transferred to the IR ellipsometer. Methyl-passivation of the Si(111) surface was carried out as follows: Additionally, the H-terminated Si (111) surface was placed in an electrochemical cell in a glove box. The applied potential was scanned from open circuit potential from −0.3 V (−0.1 V) to +2 V (2.2 V) using 0.5 M (sample # 1) and 1 M (sample # 2) CD_3MgI solved in diethylether as supplied by Sigma-Aldrich. Deuterated methyl, CD_3, was used to separate the surface modification from the signals of the adsorbed CH_3-species in the IR ellipsometry spectra. Afterwards, the Si-CD_3 sample was rinsed with water to remove adsorbed Mg salt complexes.

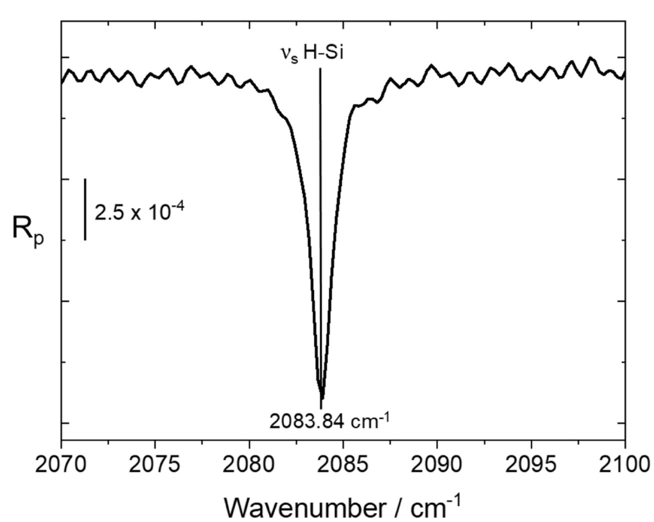

Fig. 2. Characteristic p-polarized reflection spectrum (baseline corrected) of the H/Si(111) surface at 0.5 cm^{-1} spectral resolution and 65° incidence angle.

2.2. Ellipsometry

Polarization dependent IR spectroscopic spectra were recorded using an ellipsometric set-up in a single reflection geometry attached to Fourier-transform infrared (FT-IR) spectrometer (Vertex 70 and Tensor 37, Bruker, Germany) in dry air environment (humidity < 0.25 %). The spectra were obtained with a resolution between 0.5 cm^{-1} and 4 cm^{-1} using a photovoltaic mercury–cadmium–telluride (MCT) detector (InfraRed Associates, Inc., USA) cooled with liquid nitrogen (LN_2), or with a deuterated triglycine sulfate (DTGS) detector (RT-DLaTGS, Bruker, Germany). tanΨ is defined as the ratio of amplitudes of p- and s-polarized reflection components and is calculated from the square root of the ratio of measured R_p and R_s. Further details on the method and the geometry of the experimental set-up can be found in Refs. [45,46].

2.3. Optical simulations

The basis of the used analytical optical modeling is the description of the propagation of electromagnetic waves in layered media by a 4 × 4 matrix formalism as introduced by Berreman in 1972 [47] and described by Azzam and Bashara in 1977 [48]. Specific analytical solutions can be used for isotropic and anisotropic layered systems [48,49].

For modeling of the optical response of a layered sample, the dielectric function of a material is assumed to be equal to 1 plus a sum of susceptibilities related to the specific fundamental excitations. For example, the susceptibility of a vibrational Si-H stretching excitation in the infrared spectral range can be described by a Lorentz oscillator. For further information we refer the reader to [45,46,50]. Mixtures of materials are often described by effective medium approximations (EMA) [45,46,50].

Optical modeling implemented in modern ellipsometric software is capable to fit and simulate transmission, reflection, polarimetric, and ellipsometric spectra. Here, SpectraRay/4 (Sentech Instruments GmbH, Germany) was used for all optical fits and simulations. The material of the layer was considered to be optically homogenizable, which is a reasonable assumption because the probing wavelength is much larger than structural units of the interface. However, with an infinite materials' dielectric function, potential finite island size effects cannot be separated. Beside phenomenological dipole coupling models [27] known for decades, an ab-initio based multi-scale approach was recently introduced to describe the optical response of differently sized molecular islands on dielectric substrates [51]. For our discussion, we have also considered these literature results for CO molecular finite sized islands on CeO_2 surfaces [51]. For completeness, we note that for structured surfaces with structural units in the range of the wavelengths, different kinds of numerical optical simulations of Maxwells equations can be applied, e.g., rigorous coupled-wave analysis (*RCWA*) and the finite difference time domain (*FDTD*) method.

For the optical simulations of the H-passivated surface, an anisotropic optical three-layer model was used: air/0.48 nm H-Si/Si. The Si-H vibrational band was described by a Lorentz oscillator (υ_0: resonance frequency, F: oscillator strength, Γ: damping). Further details on the optical simulations can be found in Ref [44]. The out-of-plane parameter of the initial Si-H layer in the Si-H stretching range is represented by ε_∞=1.8 [2], F=167.61 cm^{-1}, υ_0=2079.61 cm^{-1}, Γ=2.05 cm^{-1}; the in-plane component is set to ε_∞=1.8. Two types of models were used to describe the initial degradation. In the first one, the oscillator strength was reduced by about 30 % from the initial F=167.61 cm^{-1} to F=117 cm^{-1} to describe a spectrum after 1.6 days of storage. In a second model the fraction of the out-of-plane component was reduced subsequently from 100 % (initial surface) to 66 % (after 1.6 days) using an effective medium approach (EMA) in a Bruggeman model. In the simulations, the reduction of oscillator strengths aims to describe a reduction of the total amount of Si-H oscillators. The reduction of the fraction of the out-of-plane components in the EMA approach describes a reduction in the proportion of perfect domains. For the host material, ε_∞=1.8 was set.

For the optical simulations of the CD_3-functionalized surface, an anisotropic optical three-layer model was used: air/0.48 nm CD_3-Si/Si. For referencing, the experimental and simulated CD_3 spectra were divided by the simulated spectrum of the bare substrate. Only the experimental spectrum in the range of the in-plane wagging vibration is divided by a spectrum of a just degraded passivated silicon surface. An H-passivated surface cannot be used as reference here because of the overlapping Si-H bending vibration. The following parameters were used in the simulation of sample #1 (#2): υ_ρ=606.1 cm^{-1} (603.3 cm^{-1}), Γ_ρ=12.7 cm^{-1} (13.2 cm^{-1}), F_ρ=253 cm^{-1} (334 cm^{-1}); and υ_δ=972.5 cm^{-1} (974.7 cm^{-1}), Γ_δ=5.2 cm^{-1} (5.0 cm^{-1}), F_δ=114 cm^{-1} (110 cm^{-1}).

The thickness of the native oxide was evaluated from ex situ UV–VIS ellipsometric measurements (SE850, Sentech Instruments, Germany) at 20 % relative humidity. As a water layer is expected for SiO_2 surfaces [52], the thickness of the native oxide is determined to be 1.44 nm (assuming 0.6 nm water layer in the optical simulation).

2.4. Choice of detector

Highly sensitive FTIR measurements are required to study ultrathin films. The choice of the detector and related measurement parameters is crucial for optimal measurements. Beyond the optical, geometrical and electronical realization, the detector temperature, frequency dependent specific detectivity, spectral response, and noise are relevant properties. Detailed information on FTIR detector properties can be found in Ref [53]. In general, the signal to noise ratio (S/N) is proportional to the square root of the measurement time [54]. Using a DTGS detector requires long measurement times because of its low specific sensitivity. However, the low maintenance of the DTGS (no LN_2 cooling required) renders it advantageous for long-term measurements, for example, to study the band of the Si-H bending vibration. An LN_2 cooled photovoltaic MCT detector offers higher detectivity and can be used at higher sampling frequencies than a thermal DTGS detector. These MCT properties allow for fast measurements at high S/N and spectral resolutions, as required for a detailed study of the initial variations in the Si-H stretching range. The kind of detector, scan speed, spectral resolution and measurement time were carefully selected to achieve the required S/N for the respective experimental conditions and incidence angle.

2.5. Measurement conditions

R_p of H/Si(111) was measured with 0.5 cm^{-1} resolution, 65° angle of incidence, 24 min measurement time and photovoltaic MCT detector. tanΨ spectra were measured with 1 cm^{-1} resolution, 60°, 412 min measurement time, DTGS detector and 4 cm^{-1} resolution, 60° angle of incidence, ~ 24 h measurement time and DTGS detector. The H/Si(111) sample was exposed to humid air (36.8 %, 22.3 °C) for 4.5 h. Temperature and humidity were measured with a Dorstmann P770, Germany.

2.6. XPS

The sample was characterized by X-ray photoelectron spectroscopy (XPS) using a non-monochromatized MgKα source ($E = 1253.6$ eV) (XR-50 by SPECS) and a hemispherical electron analyzer (CLAM 4 by VG). The angle between source and analyzer was 54°. The base pressure of the system was 5×10^{-9} mbar. The energy calibration was performed using Cu, Ag, and Au emission lines and the pass energy was 20 eV. The peak fitting procedure was performed using Shirley backgrounds along with Gaussian–Lorentzian line shapes. The sample was stored in dry air environment (< 0.25 % humidity) for 40 days and exposed to humid air (40.5 %) for ~ 5 h.

3. Experimental results and discussion

For a better understanding of the IR spectra and their correlation to the structure of the surfaces, the vibrational spectra were recorded during the storage of the surface in dry and humid air. To interpret and identify possible initial oxidation states, XPS measurements were also performed for a pair of comparable samples. To analyze the stretching and bending mode with high S/N, the spectral resolution of the IR measurements with DTGS detector was restricted to 1 cm^{-1} and 4 cm^{-1}. In the following, we discuss the initial degradation during the first 3 days, followed by the long-term degradation over 139 days. Here, the term degradation refers to the reduction of the quality of the initial chemical surface passivation and an increase of the number of defects with time.

3.1. Degradation of the H-passivated surface

Ellipsometric tanΨ spectra (DTGS detector, 1 cm^{-1} spectral resolution) are presented in Fig. 3 as a function of time. The first measurement was immediately taken after the preparation and the last one after about 3 days storage in dry air. Using a DTGS detector allows one to access a broad spectral range including the band related to the Si-H bending vibration.

The measured spectra (Fig. 3) show a decrease of the amplitudes and increase of the full width at half maximum (FWHM) of the bands with increasing degradation. Note that –tanΨ spectra are shown in Fig. 3b for easier band comparisons. The time dependent amplitude of the band related to the bending vibration (a) is reduced much less than that of the stretching vibration (b). Therefore, we emphasize that the apparent disappearance of the band related to the H-Si stretching vibration cannot be interpreted as a complete degradation of the H-passivated surface. In the literature, a possibly related effect was also observed for strained Si (111) surfaces [29]. It was discussed that the redistribution of the bonded hydrogen in the silicon network [55] might be the reason and not a diminished hydrogen content. It is expected that both a reduced average oscillator density (top of Fig. 4a) as well as a reduction of the proportion of perfect passivated domains (defect rich areas possibly outside the perfectly passivated areas (bottom of Fig. 4a) would result in a decrease in the band amplitude. As the Si-H stretching band of a perfect H-passivated surface correlates with a strong transition dipole moment [44,56], a downwards shift of the observed band maximum by a few wavenumbers [44] would be expected for a reduction of the density of Si-H oscillators.

Fig. 4b shows the results of optical simulations for a reduction of Si-H density and the proportion of perfect domains. A decrease in oscillator strengths (Fig. 4b, top), corresponding to a reduction of Si-H oscillator density by about 30 %, leads to a clear downward shift of the band frequency (Fig. 4c). Such a shift is not observed in the experimental data. However, the data can be understood in terms of the scenario depicted at the bottom of Fig. 4b Here the simulated spectra reflect a reduction in the proportion of perfect domains by approximately 34 %, which captures the time-development of the shift in the measured spectra (Fig. 4c). In Fig. 4d, the relative reduction of oscillator strengths and proportion of perfect domains with time are compared to the time-dependent development of the measured band amplitudes. Both simulated scenarios predict a similar decrease in band amplitude, but at a much slower rate than observed experimentally. This finding shows that, for the initial degradation of the sample, correlating the measured Si-H stretching band amplitudes and shifts with oscillator density or the proportion of perfect domains is only possible with the support of optical simulations.

In Fig. 3 it was observed that the Si-H stretching vibration only shifts by about 0.6 cm^{-1} (indicated by the dotted vertical lines in Fig. 3b) until the amplitude is reduced to the noise level. The maximum possible shift for this band would be about 4.2 cm^{-1} as calculated from the difference of the observed Si-H resonance (2083.84 cm^{-1}) and the Si-H resonance used for simulations (2079.61 cm^{-1}). For the Si-H stretching band in p-polarized spectra, this shift corresponds to the difference between the resonances of a surface with ideally covered terrasses and a surface covered with well-separated single oscillators. For a layer with tilted

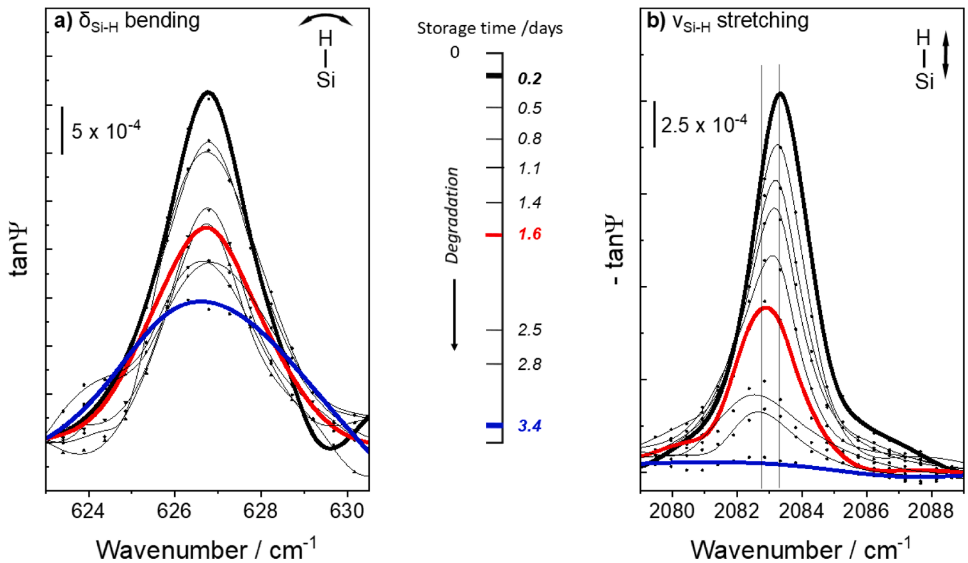

Fig. 3. Initial degradation of the H-Si surface in dry air (< 0.25 % humidity). Baseline corrected ellipsometric tanΨ spectra at 1 cm^{-1} spectral resolution for a) Si-H bending vibration, b) Si-H stretching vibration. To better visualize the differences of the variations of the bands during degradation in a) and b), the initial band and those after 1.6 days and after 3.4 days are shown as thick lines in black, red and blue, respectively.

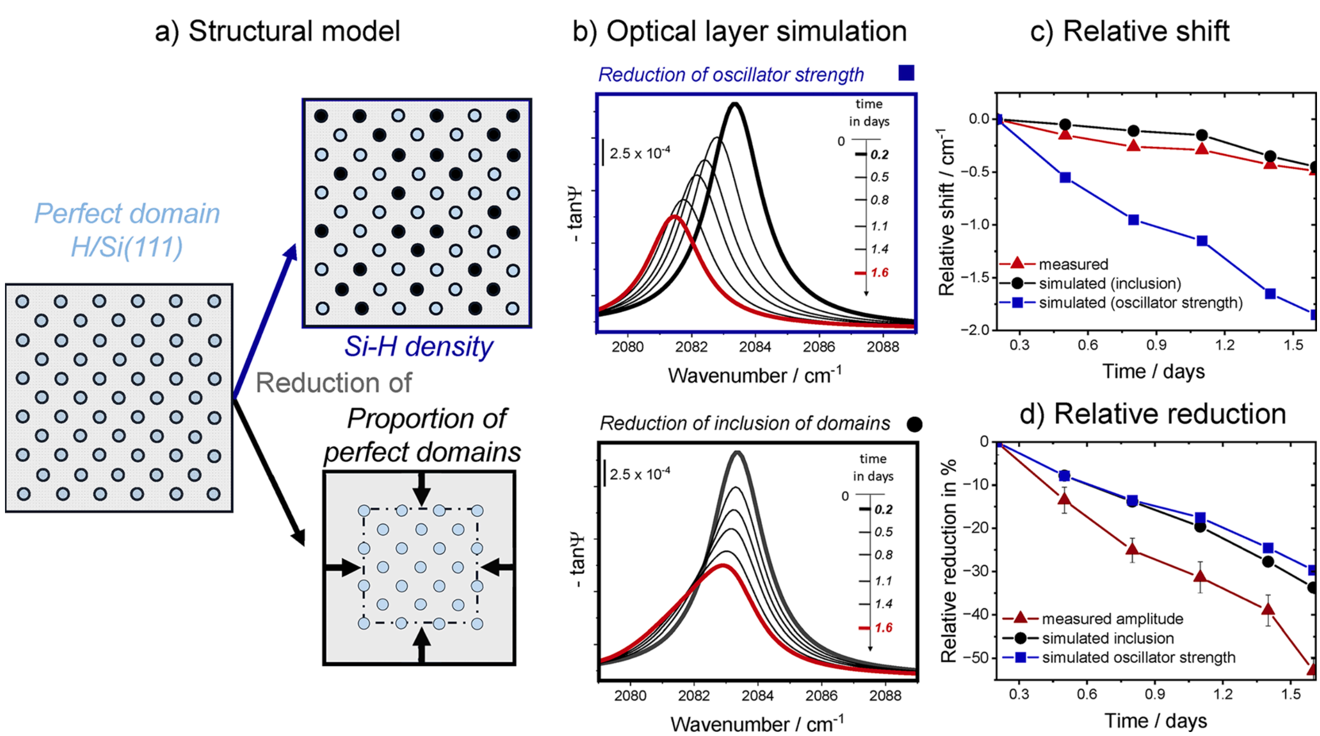

Fig. 4. Schematic scenarios a) structural model, b) optical model for the pathway of degradation of perfect H-Si(111) domains leading to a time dependent reduction of band amplitudes (30 % of the initial H-passivated surface is expected to be covered with perfect (1 × 1) domains containing about 5000 Si-H oscillators [27]); a) structural models are shown. Top: an initially completely H-passivated surface (blue spheres, left side) is degrading with time by the formation of randomly distributed defects (black spheres); Bottom: with time, the proportion of perfect domains is reduced. b) The results of optical simulations of tanΨ spectra (Fig. 3b) are shown. Top: A model reducing oscillator strengths represents the random increase of defects. Bottom: an EMA model displays the varying number of inclusions representing a reduced contribution of domains. c) Relative shift of the simulated band maxima for reduction of oscillator strength (related to Si-H density) and proportion of perfect domains from simulations in b) and relative shift of measured band maxima. d) Corresponding reduction of the measured amplitudes and the simulated inclusions and oscillators strengths.

dipoles, such a shift could in principle also be observed directly by the difference of the band frequency in p- and s-polarized spectra. Because the transition dipole moment (TDM) of the Si-H stretching vibration is perpendicular to the surface (no contribution in s-polarized spectra), this approach is not accessible for the passivated Si(111) surface. However, in a literature study of a CO monolayer with tilted molecules, the shift was directly measured by the difference of the related band frequency in p- and s-polarized spectra [51]. Interestingly, a comparable shift of 4 cm^{-1} was found. The experiments were complemented by ab-initio based multiscale optical calculations to understand potential contributions related to the occurrence of finite-sized islands [51]. To illustrate this context, Fig. 5 shows the simulated relative shift of a band related to CO oscillators in dependence of varying molecular island size as adapted from Ref [51].

Fig. 5 shows that the band shift for sizes of 10 nm x 10 nm already converges towards the shift expected for an infinite system [51]. A shift of about 0.6 cm^{-1} could be correlated with a reduction of the island size to about 4 nm x 4 nm. A related effect for our surfaces indicates that the size of the perfect domains remains above a minimum size. However, a shrinking of initially large domains to a size of about 4 nm x 4 nm would result in a too low proportion of the areas of perfect domains. On the other hand, a separation of larger domains into several smaller ones could still be a scenario that cannot be excluded by our optical simulations.

In conclusion, we assign the strongly diminishing amplitude and the weak shift observed with ongoing degradation to a strong decrease in the total amount of the perfectly passivated areas, possibly accompanied by a shrinking size of the domains. In our experiments, the band amplitude of the sharp Si-H stretching mode is within the experimental noise after 3 days, meaning that the number of perfectly passivated domains with a minimum size of a few nm becomes negligible. The optical interpretation (details in the methods section) indicates that the effective dielectric function of the Si-H surface layer now shows the characteristics of a weak oscillator (k ∼< 0.4 and no ε_r near zero condition). However, at the same time, the band of the bending mode is clearly visible after 3 days of degradation. This can only be explained for a condition where hydrogen was not removed for the majority of defects. To study this point in more detail, we investigated the long-term degradation.

3.2. Long term degradation of the H-passivated Si(111) surface

Further measurements were performed at 4 cm^{-1} spectral resolution (Fig. 6) in order to reveal with sufficient S/N the background in the Si-H stretching region. Fig. 6 shows IR spectra in a) the Si-H bending region, b) the SiO_x and c) the Si-H stretching range after degradation for 1, 6, 41, 107, and 139 days in dry air, followed by the additional exposure to humid environment for 4.5 h. The IR spectra after 1 day show characteristic bands related to Si-H vibrations, but no considerable peak in the SiO_x range. The spectra after further degradation reveal a much broader and much weaker band below the sharp Si-H peak. A possible assignment of this band is to a contribution of less ordered Si-H passivated areas and/or contributions of perfectly passivated Si-H domains smaller than a few nm. For stepped and nanorough surfaces, vibrational contributions are also expected in this spectral range [39]. However, no distinct and significant band contributions related to SiH_2 can be identified in our experiments (see also Fig. S1 in the supplementary). With the ongoing degradation, the reduced amplitudes of the Si-H bending mode qualitatively correlate with those of the broad band in the Si-H stretching range. After 41 days of storage (green spectra) in dry air, bands related to Si-H vibrations are still observed and a weak SiO_x related peak is already seen. With further dry air storage of 139 days, the amplitudes of the Si-H related peaks in the IR spectra decrease and the amplitude of the SiO_x related peak increases. After subsequent exposure to humid air for a few hours, the residual bands related to bending and stretching S-H vibrations disappear and the SiO_x related peak increases significantly. However, even after the exposure to humid air, the band maximum in the IR spectra is not yet shifted to values typical for a closed SiO_2 layer (∼ 1240 cm^{-1}).

For comparison, XPS data are presented in Fig. 7 after storage for 40 days in dry air (top) and additional exposure to humid environment for 5 h (bottom). A weak contribution of Si^{1+}(∼100.8 eV) can be observed in the Si 2p-XP spectrum for a sample stored for 40 days in dry air (Fig. 7, top spectrum) in addition to the Si $2p_{3/2}$ (∼99.3 eV) and Si $2p_{1/2}$ (∼99.9 eV) components. From this finding, it can be concluded that the oxidation of the surface has started, but no severe surface oxidation has occurred yet. After exposure for 5 h to humid air the XPS spectra show Si^{4+} (∼102.9 eV) contributions related to parts of fully coordinated SiO_2 (see Fig. 7, bottom spectrum). The presence of a Si^{4+} state indicates that the surface has been only partially oxidized. For a monolayer of oxide, a larger Si^{4+} amplitude would be expected [31].

The XPS results are in general agreement with the interpretation of the IR data in Fig. 6**,** identifying a weak band in the SiO_x range after 41 days of storage in dry air and a stronger peak in this range after exposure to humid air. In summary, it can be concluded that even after 40 days of dry air storage, no severe oxidation has occurred. Furthermore, after exposure to humid air for a few hours, the interface is partially oxidized but has not formed a closed SiO_2 layer. The finding indicates a non-uniform oxidation for the Si(111) surface, which is in qualitative agreement with findings in Ref [31].

3.3. Application to molecular functionalized silicon surfaces

Oxide-free H-terminated silicon surfaces functionalized with molecular monolayers can be used for passivation but also to tune the interface properties [2] toward a wide range of applications from electronics to photovoltaics [7]. For example, alkyl monolayers (-CH_3, -CD_3) on Ge(111) and Si(111) prepared by a halogenation/alkylation process have been studied in detail by IR spectroscopy [57] and references therein]. In the following, ellipsometric IR spectra of a CD_3 monolayer on Si(111) are discussed as an exemplary example for promising future research and analysis applications in this field. tanΨ spectra of a CD_3 functionalized Si(111) surface are displayed in Fig. 8a for two different preparations (see 2.1, sample # 1 and sample # 2). As with the H-passivated Si(111) surface, a direct visual inspection of the polarimetric spectrum allows the identification of bands with opposite TDMs,

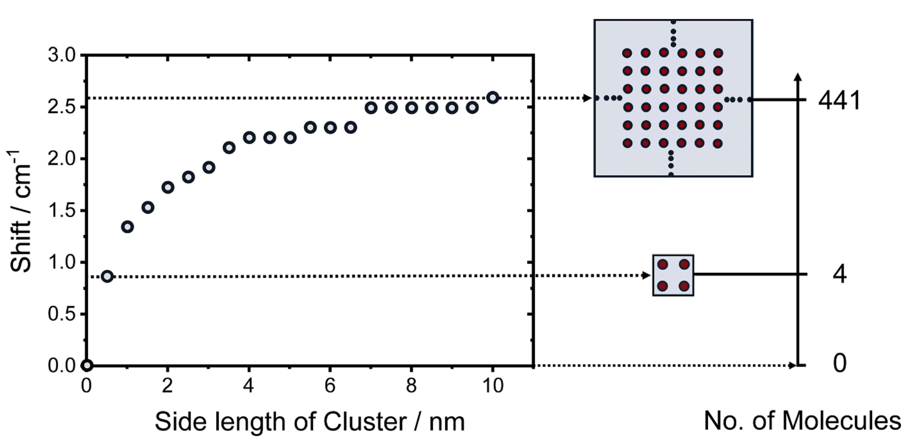

Fig. 5. Simulated band shift in p-polarized spectra for finite sized CO molecular islands, adapted from Ref [51].

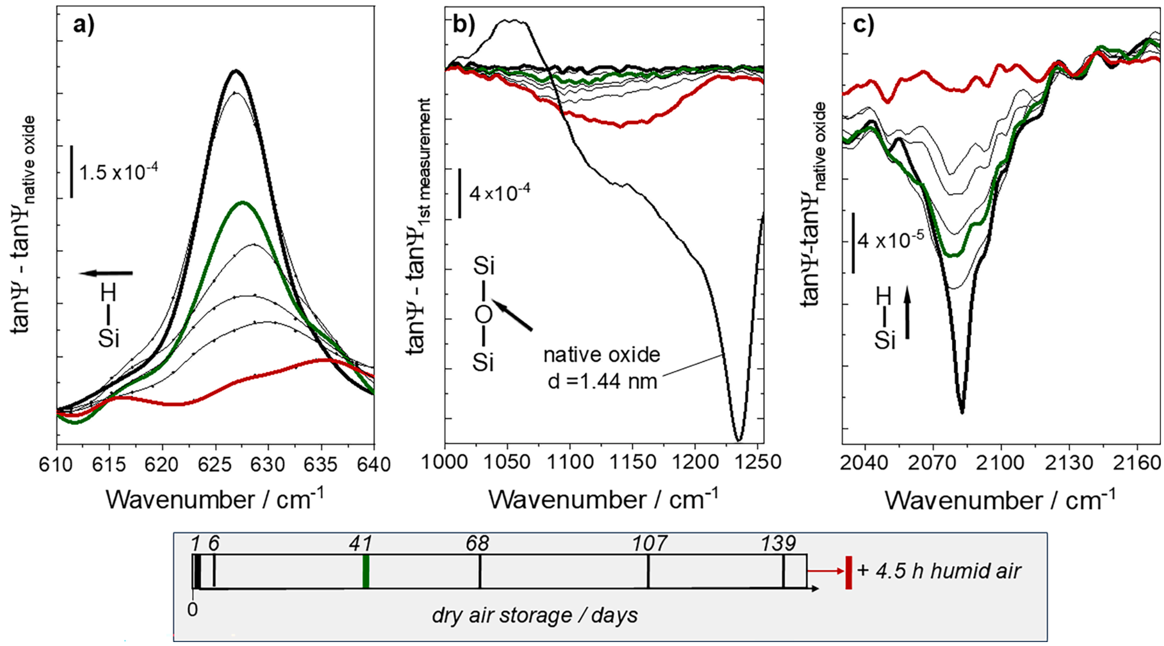

Fig. 6. Referenced baseline corrected IR spectra of H/Si(111) during long-term degradation in dry air and subsequent exposure to humid air for 4.5 h. Spectral ranges of a) Si-H bending, b) SiO_x stretching, c) Si-H stretching vibrations. The spectrum of a native SiO_2 film with a thickness of 1.44 nm (initial surface before the passivation) as shown in b) was used for referencing in a) and c). The timeline is shown below. The days of measurements are indicated, the spectrum after one day is represented by a thick black line, the one after exposure to humid air is represented by a thick red line, and the spectrum after 41 days storage is represented by a thick green line.

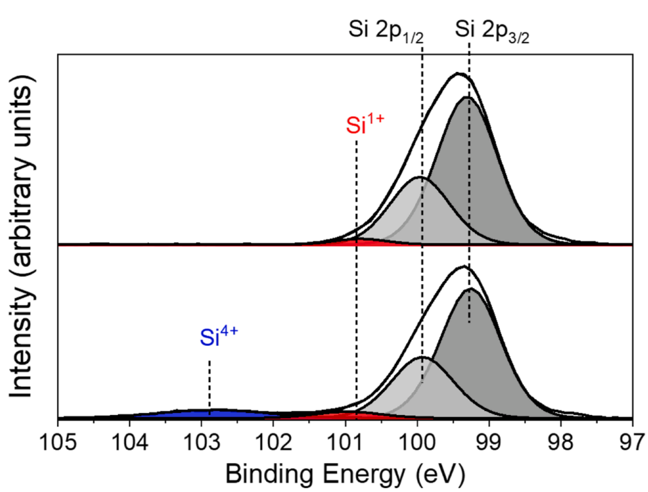

Fig. 7. XPS spectra in the Si 2p range for a sample after 40 days storage in dry air (top), followed by 5 h exposure to humid air (bottom) together with the fitted components Si^{4+} and Si^{1+} (spin-orbit coupling not resolved), Si $2p_{1/2}$ and Si $2p_{3/2}$ for elemental Si.

evident from the upward (in-plane) and downward pointing (out-of--plane) peaks.

As discussed later, an optical simulation determining the oscillator parameters (frequencies, halfwidths and strengths), can then serve for more a detailed study of the monolayer far beyond the bare possibility of identification.

From literature [57], the following positions and line widths are expected for CD_3-Si(111): 604 cm^{-1} (12–13 cm^{-1}) and 979 cm^{-1} (4–5 cm^{-1}) for ρ (in-plane wagging) and δ (out-of-plane umbrella) vibrations, respectively. In our experiments for a CD_3 monolayer on a highly doped Si(111) surface (Fig. 8), band maxima read-out from the spectra are at 607 cm^{-1} (603.5 cm^{-1}) and at 975.4 cm^{-1} (977.6 cm^{-1}) for sample # 1 (sample #2). In comparison with the literature values (with 4 cm^{-1} spectral resolution, [57]) differences in the range of a few wavenumbers are seen for the observed band position; for the band widths, similar values are observed compared to the data in Refs [35,57].

In contrast to the direct read-out of band frequencies, an optical simulation can determine the exact oscillator parameters (see also Section 2.3). An optical layer simulation (air/0.48 nm CD_3-Si/Si) then delivers the optical constants (Fig. 8b). Notably, for the out-of-plane mode, the simulated resonance frequency (indicated by dashed lines in Fig. 8a and b) is about 3.5 cm^{-1} lower than the read-out frequency. The shift is slightly smaller than that observed for the Si-H stretching mode, yet it still reflects the characteristics of a strong oscillator. The simulations also reveal that the oscillator strengths of the in-plane wagging mode are about a factor of 2-3 stronger than the one of the out-of-plane umbrella vibration. However, because the TDM is in-plane oriented, the simulated resonance frequency and the read-out frequency are similar.

It is important to note that the directly read-out band positions for the out-of-plane related band are different to the resonance frequencies determined from the optical simulation. The observed difference of these band frequencies of a few wavenumbers is expected for bands related to strong out-of-plane transition dipole moments with decreasing average transition dipole moments. This could arise e.g. for a decreasing density of oscillators [44] (similarly to the scenario displayed at the top of Fig. 4a). For the two different preparations (#1 and #2, Fig. 8), the simulated resonance frequencies of the umbrella mode differ by about 2.2 cm^{-1}. This could indicate a slightly lower average density of oscillators for the present preparations. However, as the literature values [35,57] were measured with 4 cm^{-1} resolution, a direct comparison to our 1 cm^{-1} measurements is only possible to a limited extend for the bands with small FWHM (see also Figure S2 in the supplementary). For a purely density-driven effect, a varying band frequency and amplitude would be expected, similar as discussed in Fig. 4b. However, the measured data in Fig. 8 show no amplitude variation for the $\delta_{\perp}$ mode, but for the $\rho_{\|}$ mode. Also a significant shift of approximately 3.5 cm^{-1} is detected for the in-plane oriented mode for the two samples. This indicates that, in addition to the discussed density effects, influencing the frequency, also other physical effects contribute.

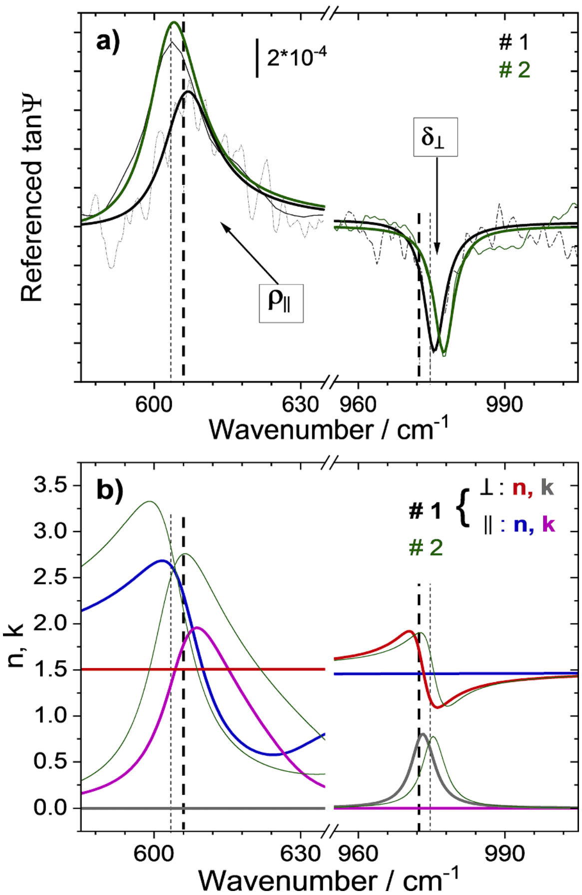

Fig. 8. a) Referenced experimental and simulated tanΨ spectra (1 cm^{-1} spectral resolution) of the CD_3/Si(111) surface (sample # 1 and sample #2). Characteristic bands related to in-plane and out-of-plane vibrations are marked. Results of an optical layer simulation are shown as thick lines. The green spectra correspond to a sample with different preparation (sample # 2). It was measured with better signal to noise ratio (DTGS with 4 cm^{-1} resolution in the lower range and MCT, 1 cm^{-1} resolution in the higher frequency range). b) Simulated optical constants n and k. Dashed lines indicate the resonance frequencies as determined by the optical simulation.

In summary, this subsection demonstrated that optical simulations closely match the read-out frequencies for the in-plane mode, whereas notable discrepancies of several wavenumbers are observed for the out-of-plane mode. For the CD_3/Si(111) sample, these results, along with the observed frequency differences between the two preparations, suggest a complex scenario involving physical effects from local imperfections, varying molecular density and possible adsorbates. However, this finding was only achievable through the use of high spectral resolution over a broad spectral range, combined with optical simulations to interpret the experimental data. Relying solely on the analysis of a single band without optical simulations could lead to incorrect conclusions. Ongoing research on these surfaces focuses, e.g., on the optimization of such methyl monolayers in dependence of different electrochemical preparation conditions.

4. Conclusions

In this work it has been demonstrated that a pair of in-plane and out-of-plane oriented vibrations allows one to investigate the degree of passivation and degradation. The narrow bands related to out-of-plane directed Si-H stretching vibrations with a strong transition dipole moment are sensitive to amount and size of well-ordered domains but cannot be used to conclude on the overall passivation of the surface. For such a purpose, either the band related to in-plane bending vibrations or in addition a broad band in the range of the Si-H stretching vibrations should be taken into account. However, because of its low amplitude (lower than ~ 0.00015), this broad band in the spectral range of the Si-H stretching vibrations can be easily overlooked in spectrally highly resolved measurements. From a detailed discussion of the IR spectra that include optical simulations, quantitative conclusions on the reduction of the proportion of the initially perfectly passivated domains can be drawn. The data also show that a large proportion of the surface is not passivated by perfect Si-H domains and that oxidation of the surface is non-uniform. In summary, our investigation shows that a pair of anisotropic bands, particularly the interpretation of bands related to out-of-plane vibrations with strong transition dipole moments, can serve for detailed structural and morphological interpretations by accompanying optical simulations. This analytic approach is feasible and useful in the analysis of molecular interfaces, which is exemplarily shown for methyl monolayers on Si(111). Future application of such approaches could be also the usage in parallel broadband IR and soft X-rays radiation analyses, e.g. at the ELISA beamline at BESSY II in Berlin [58], which can enable analyses with temporal and spatial overlap.

CRediT authorship contribution statement

Karsten Hinrichs: Writing – review & editing, Writing – original draft, Visualization, Validation, Resources, Project administration, Methodology, Investigation, Funding acquisition, Formal analysis, Data curation, Conceptualization. **Fatima Akhtar:** Writing – original draft, Validation, Methodology, Investigation, Formal analysis, Data curation. **Merve Buldu-Akturk:** Methodology. **Andreas Furchner:** Writing – review & editing, Writing – original draft, Resources, Methodology. **Iver Lauermann:** Writing – review & editing, Resources, Methodology, Investigation. **Norbert H. Nickel:** Writing – review & editing, Writing – original draft, Visualization, Methodology. **Jörg Rappich:** Writing – review & editing, Writing – original draft, Validation, Resources, Methodology, Investigation, Data curation, Conceptualization.

Declaration of competing interest

The authors declare the following financial interests/personal relationships which may be considered as potential competing interests:

Karsten Hinrichs reports financial support was provided by European Union. Joerg Rappich reports financial support was provided by European Union. Karsten Hinrichs reports financial support was provided by Senate of Berlin Department of Science Health and Care. Karsten Hinrichs reports financial support was provided by Federal Ministry of Education and Research. If there are other authors, they declare that they have no known competing financial interests or personal relationships that could have appeared to influence the work reported in this paper.

Acknowledgements

The authors thank Özgür Savaş and Ilona Engler for technical support. We acknowledge the financial support by the Europäischer Fonds für regionale Entwicklung (EFRE) (1.8/13 and *Pro* FIT 10185407); the Senatsverwaltung für Wissenschaft, Gesundheit und Pflege des Landes Berlin and the Federal Ministry of Education and Research.

Supplementary materials

Supplementary material associated with this article can be found, in the online version, at doi:10.1016/j.apsadv.2025.100869.

Data availability

Data will be made available on reasonable request.

References

[1] P. Dumas, Y.J. Chabal, R. Gunther, A. Taleb Ibrahimi, Y. Petroff, Vibrational characterization and electronic properties of long range-ordered, ideally hydrogen-terminated Si(111), Prog. Surf. Sci. 48 (1995) 313–324, https://doi.org/10.1016/0079-6816(95)93437-C.

[2] P. Jakob, Y.J. Chabal, Krishnan Raghavachari, P. Dumas, S.B. Christman, Imperfections on the chemically prepared, ideally H-terminated Si(111)-(1 × 1) surfaces, Surf. Sci. 285 (1993) 251–258, https://doi.org/10.1016/0039-6028(93)90436-N.

[3] G.S. Higashi, Y.J. Chabal, G.W. Trucks, Krishnan Raghavachari, Ideal hydrogen termination of the Si (111) surface, Appl. Phys. Lett. 56 (1990) 656–658, https://doi.org/10.1063/1.102728.

[4] K. Itaya, R. Sugawara, Y. Morita, H. Tokumoto, Atomic resolution images of H-terminated Si(111) surfaces in aqueous solutions, Appl. Phys. Lett. 60 (1992) 2534–2536, https://doi.org/10.1063/1.106904.

[5] S.P. Pujari, A.D. Filippov, S. Gangarapu, H. Zuilhof, High-density modification of H-terminated Si(111) surfaces using short-chain alkynes, Langmuir 33 (2017) 14599–14607, https://doi.org/10.1021/acs.langmuir.7b03683.

[6] J. Veerbeek, N.J. Firet, W. Vijselaar, R. Elbersen, H. Gardeniers, J. Huskens, Molecular monolayers for electrical passivation and functionalization of silicon-based solar energy devices, ACS. Appl. Mater. Interfaces 9 (2017) 413–421, https://doi.org/10.1021/acsami.6b12997.

[7] J. Veerbeek, J. Huskens, Applications of monolayer-functionalized H-terminated. Silicon surfaces: a review, Small. Methods 1 (2017) 1700072, https://doi.org/10.1002/smtd.201700072.

[8] D.J. Michalak, S.R. Amy, D. Aureau, M. Dai, A. Estève, Y.J. Chabal, Nanopatterning Si(111) surfaces as a selective surface-chemistry route, Nat. Mater. 9 (2010) 266–271, https://doi.org/10.1038/nmat2611.

[9] M. Sajjad, X. Yang, P. Altermatt, N. Singh, U. Schwingenschlögl, S. De Wolf, Metal-induced gap states in passivating metal/silicon contacts, Appl. Phys. Lett. 114 (2009) 071601, https://doi.org/10.1063/1.5066423.

[10] E.C. Wurst, E.H. Borneman, Rectification properties of metal-silicon contacts, J. Appl. Phys. 28 (1957) 235–240, https://doi.org/10.1063/1.1722713.

[11] Y.C. Yu, E.H. Snow, Minority carrier injection of metal-silicon contacts, Solid. State Electron. 12 (1969) 155–160, https://doi.org/10.1016/0038-1101(69)90027-6.

[12] L. Korte, E. Conrad, H. Angermann, R. Stangl, M. Schmidt, Advances in a-Si:h/c-Si heterojunction solar cell fabrication and characterization, Sol. Energy Mater. Sol. Cells 93 (2009) 905–910, https://doi.org/10.1016/j.solmat.2008.10.020.

[13] J.I. Michel, J. Dréon, M. Boccard, J. Bullock, B. Macco, Carrier-selective contacts using metal compounds for crystalline silicon solar cells, Prog. Photovolt Res. Appl. 31 (2023) 380–413, https://doi.org/10.1002/pip.3552.

[14] M. Lozac'h, S. Nunomura, Role of silicon surface, polished ⟨100⟩ and ⟨111⟩ or textured, on the efficiency of double-sided TOPCon solar cells, Prog. Photovolt Res. Appl. 28 (2020) 1001–1011, https://doi.org/10.1002/pip.3304.

[15] K. Nakano, T. Uto, D. Adachi, M. Kanematsu, H. Uzu, et al., Silicon heterojunction solar cell with interdigitated back contacts for a photoconversion efficiency over 26%, Nat. Energy 2 (2017) 17032.

[16] F. Owman, P. Mårtensson, STM study of Si(111)1×1-H surfaces prepared by in situ hydrogen exposure, Surf. Sci. 303 (1994) L367–L372, https://doi.org/10.1016/0039-6028(94)90772-2.

[17] J. Pitters, J. Croshaw, R. Achal, L. Livadaru, S. Ng, R. Lupoiu, T. Chutora, T. Huff, K. Walus, R.A. Wolkow, Atomically precise manufacturing of silicon electronics, ACS. Nano 18 (2024) 6766–6816, https://doi.org/10.1021/acsnano.3c10412.

[18] P. Constantinou, T.J.Z. Stock, L.T. Tseng, D. Kazazis, M. Muntwiler, C.A.F. Vaz, Y. Ekinci, G. Aeppli, N.J. Curson, S.R. Schofield, EUV-induced hydrogen desorption as a step towards large-scale silicon quantum device patterning, Nat. Commun. 15 (2024) 694, https://doi.org/10.1038/s41467-024-44790-6.

[19] G.W. Trucks, Krishnan Raghavachari, G.S. Higashi, Y.J. Chabal, Mechanism of HF etching of silicon surfaces: a theoretical understanding of hydrogen passivation, Phys. Rev. Lett. 65 (1990) 504–507, https://doi.org/10.1103/PhysRevLett.65.504.

[20] R. Honke, A.P. Mayer, P. Pavone, U. Schröder, Theoretical investigation of the surface dynamics of Si(111):H-(1×1), Surf. Sci. 377-379 (1997) 317–320, https://doi.org/10.1016/S0039-6028(96)01390-8.

[21] U. Harten, J.P. Toennies, Ch. Wöll, L. Miglio, P. Ruggerone, L. Colombo, G. Benedek, Surface phonons in Si(111) + H(1×1), Phys. Rev. B 38 (1988) 3305–3310, https://doi.org/10.1103/PhysRevB.38.3305.

[22] R.B. Doak, Y.J. Chabal, G.S. Higashi, P. Dumas, Inelastic helium scattering measurements of surface phonons in hydrogen-terminated Si(111) (1 × 1), J. Electron. Spectros. Relat. Phenom. 54-55 (1990) 291–298, https://doi.org/10.1016/0368-2048(90)80221-U.

[23] Ch. Stuhlmann, G. Bogdányi, H. Ibach, Surface phonons of the hydrogen-terminated Si(111)(1×1) surface, Phys. Rev. B 45 (1992) 6786–6792, https://doi.org/10.1103/PhysRevB.45.6786.

[24] H. Kato, T. Taoka, S. Suto, S. Nishikata, G. Sazaki, K. Nakajima, T. Yamada, R. Czajka, A. Wawro, A. Kasuya, Preparation and characterization of Ultraclean H: si(.111)-(1x1) surfaces studied by HREELS, AFM and STM-STS, e-J. Surf. Sci. Nanotechnol. 7 (2009) 557–562, https://doi.org/10.1380/ejssnt.2009.557.

[25] Y. Caudano, P.A. Thiry, Y.J. Chabal, Investigation of the bending vibrations of vicinal H/Si(111) surfaces by infrared spectroscopy, Surf. Sci. 502-503 (2002) 91–95, https://doi.org/10.1016/S0039-6028(01)01904-5.

[26] S. Watanabe, M. Shigeno, N. Nakayama N. Nakayama, T. Ito, Silicon-monohydride termination of Silicon-111 surface formed by boiling water, Jpn. J. Appl. Phys. 30 (1991) 3575, https://doi.org/10.1143/JJAP.30.3575.

[27] P. Jakob, Y.J. Chabal, Krishnan Raghavachari, Lineshape analysis of the Si-H stretching mode of the ideally H-terminated Si(111) surface: the role of dynamical dipole coupling, Chem. Phys. Lett. 187 (1991) 325, https://doi.org/10.1016/0009-2614(91)90433-A.

[28] P. Jakob, Y.J. Chabal, K. Kuhnke, S.B. Christman, Monohydride structures on chemically prepared silicon surfaces, Surf. Sci. 302 (1994) 49–56, https://doi.org/10.1016/0039-6028(94)91095-2.

[29] T.M. Hafshejani, J. Wohlgemuth, P. Thissen, Strain activation of surface chemistry on H-terminated Si(111), J. Phys. Chem. C 125 (2021) 19811–19820, https://doi.org/10.1021/acs.jpcc.1c06309.

[30] G.A. Ferguson, K. Raghavachari, D.J. Michalak, Y. Chabal, Adsorbate−surface phonon interactions in deuterium-passivated Si(111)-(1 × 1), J. Phys. Chem. C 112 (2008) 1034–1039, https://doi.org/10.1021/jp0758768.

[31] T. Hattori, T. Aiba, E. Iijima, Y. Okube, H. Nohira, N. Tate, M. Katayama, Initial stage of oxidation of hydrogen-terminated silicon surfaces, Appl. Surf. Sci. 104-105 (1996) 323–328, https://doi.org/10.1016/S0169-4332(96)00165-1.

[32] C.G.T. Feugmo, B. Champagne, Y. Caudano, F. Cecchet, Y.J. Chabal, V. Liégeois, Towards modelling the vibrational signatures of functionalized surfaces: carboxylic acids on H–Si(111) surfaces, J. Phys.: Condens. Matter 24 (2012) 124111, https://doi.org/10.1088/0953-8984/24/12/124111.

[33] J. Hänisch, K. Hinrichs, J. Rappich, Surface functionalization toward biosensing via free-standing Si–OH bonds on nonoxidized silicon surfaces, ACS. Appl. Mater. Interfaces. 11 (2019) 31434–31440, https://doi.org/10.1021/acsami.9b03583.

[34] F. Yang, R. Hunger, K. Roodenko, K. Hinrichs, K. Rademann, J. Rappich, Vibrational and electronic characterization of ethynyl derivatives grafted onto hydrogenated Si(111) surfaces, Langmuir. 25 (2009) 9313–9318, https://doi.org/10.1021/la900871g.

[35] F. Yang, K. Roodenko, R. Hunger, K. Hinrichs, K. Rademann, J. Rappich, Near-ideal complete coverage of CD3 onto Si(111) surfaces using one-step electrochemical grafting: an IR ellipsometry, synchrotron XPS, and photoluminescence study, J. Phys. Chem. C 116 (2012) 18684–18690, https://doi.org/10.1021/jp301013t.

[36] K. Roodenko, J. Rappich, M. Gensch, N. Esser, K. Hinrichs, Studies of electrochemically grafted thin organic layers on inorganic surfaces with infrared spectroscopic ellipsometry, Appl. Phys. A 90 (2008) 175–178, https://doi.org/10.1007/s00339-007-4251-y.

[37] J. Rappich, K. Hinrichs, In situ study of nitrobenzene grafting on Si(1 1 1)-H surfaces by infrared spectroscopic ellipsometry, Electrochem. Comm. 11 (2009) 2316–2319, https://doi.org/10.1016/j.elecom.2009.10.014.

[38] K. Roodenko, J. Rappich, F. Yang, X. Zhang, N. Esser, K. Hinrichs, Anisotropy in hydrogen-passivated and organically modified nanoporous silicon surfaces studied by polarization dependent IR spectroscopy, Langmuir 25 (2009) 1445–1452, https://doi.org/10.1021/la802685m.

[39] J. Holovský, J. Šebera, V. Sychrovský, J. Zemen, S. De Wolf, C. Ballif, Quantitative analysis of nanorough hydrogenated Si(111) surfaces through vibrational spectral assignment by periodic DFT calculations, J. Phys. Chem. C 126 (2022) 8278–8286, https://doi.org/10.1021/acs.jpcc.1c09766.

[40] V. Burrows, Y.J. Chabal, G.S. Higashi, K. Raghavachari, S.B. Christman, Infrared spectroscopy of Si(111) surfaces after HF treatment: hydrogen termination and surface morphology, Appl. Phys. Lett. 53 (1988) 998, https://doi.org/10.1063/1.100053.

[41] M. Niwano, J. Kageyama, K. Kurita, K. Kinashi, I. Takahashi, N. Miyamoto, Infrared spectroscopy study of initial stages of oxidation of hydrogen-terminated Si surfaces stored in air, J. Appl. Phys. 76 (1994) 2157–2163, https://doi.org/10.1063/1.357627.

[42] P. Jakob, Y.J. Chabal, Chemical etching of Vicinal Si(111): dependence of the surface structure and the hydrogen termination on the pH of the etching solutions, J. Chem. Phys. 95 (1991) 2897–2909, https://doi.org/10.1063/1.460892.

[43] K. Hinrichs, M. Gensch, N. Esser, Analysis of organic films and interfacial layers by infrared spectroscopic ellipsometry, Appl. Spectrosc. 59 (2005) 272A, https://doi.org/10.1366/000370205774783106.

[44] K. Hinrichs, N. Shetty, S. Kubatkin, P. Malmberg, S. Lara-Avila, A. Furchner, J. Rappich, Field manipulation of band properties in infrared spectra of thin films, Adv. Photonics Res. 5 (2024) 2300212, https://doi.org/10.1002/adpr.202300212.

[45] K. Hinrichs, K.-J. Eichhorn (Eds.), Ellipsometry of Functional Organic Surfaces and Films, Springer Nature, 2018, https://doi.org/10.1007/978-3-319-75895-4. Springer Series of. Surface Science. Vol. 52.

[46] A. Röseler, E.H. Korte, Chap. 2.8: infrared spectroscopic ellipsometry, in: J. M. Chalmers, P.R. Griffiths (Eds.), Handbook of Vibrational Spectroscopy, John Wiley & Sons, Ltd, 2001, https://doi.org/10.1002/0470027320.s2208.

[47] D.W. Berreman, Optics in stratified and anisotropic Media: 4×4-matrix formulation, J. Opt. Soc. Am. 62 (1972) 502–510.

[48] R.M.A. Azzam, N.M. Bashara, Ellipsometry and Polarized Light, North Holland Publishing Company, 1977.

[49] M. Schubert, Polarization-dependent optical parameters of arbitrarily anisotropic homogeneous layered systems, Phys. Rev. B 53 (1996) 4265–4274. https://link.aps.org/doi/10.1103/PhysRevB.53.4265.

[50] H.G. Tompkins, E.A. Irene (Eds.), Handbook of Ellipsometry, William Andrews Publications, Norwich, NY, 2005.

[51] B. Zerulla, M. Krstić, S. Chen, Z. Yu, D. Beutel, C. Holzer, M. Nyman, A. Nefedov, Y. Wang, T.G. Mayerhöfer, C. Wöll, C. Rockstuhl, Polarization-dependent effects in vibrational absorption spectra of 2D finite-size adsorbate islands on dielectric substrates, Phys. Chem. Chem. Phys. 26 (2024) 13683–13693, https://doi.org/10.1039/D4CP00860J.

[52] A. Verdaguer, C. Weis, G. Oncins, G. Ketteler, H. Bluhm, M. Salmeron, Growth and structure of water on SiO2 films on Si investigated by Kelvin probe microscopy and in situ X-ray spectroscopies, Langmuir 23 (2007) 9699–9703, https://doi.org/10.1021/la700893w.

[53] W. l. Wolfe, G.J. Zissis (Eds.), The Infrared Handbook, By The Infrared Information Analysis (IRIA) Center, Environmental Research Institute of Michigan, 1993, 4th printing.
[54] P.R. Griffiths, J.A. de Haseth (Eds.), Fourier Transform Infrared Spectrometry, John Wiley & Sons, Inc., Hoboken, New Jersey, 2007, https://doi.org/10.1002/9780470106310.
[55] R. Darwich, P.R.I. Cabarrocas, S. Vallon, R. Ossikovski, P. Morin, K. Zellama, Observation by infrared transmission spectroscopy and infrared ellipsometry of a new hydrogen bond during light-soaking of a-Si:H, Philos. Mag. B 72 (1995) 363–372, https://doi.org/10.1080/13642819508239090.
[56] W. Henrion, A. Roeseler, H. Angermann, M. Rebien, Application of UV-VIS and FTIR spectroscopic ellipsometry to the characterization of wet-chemically treated Si surfaces, Phys. Status Solidi A 175 (1999) 121–128, https://doi.org/10.1002/(SICI)1521-396X(199909)175:1≤121::AID-PSSA121≥3.0.CO;2-D.
[57] D. Knapp, B.S. Brunschwig, N.S. Lewis, Transmission infrared spectra of CH3–, CD3–, and C10H21–Ge(111) surfaces, J. Phys. Chem. C 115 (2011) 16389–16397, https://doi.org/10.1021/jp110550t.
[58] S. Vadilonga, P. Dumas, U. Schade, K. Holldack, K. Hinrichs, G. Reichardt, T. Gerber, J.P.Hofmann A.Vollmer, H. Oertel, B. Rech, R. Schlögl, J. Viefhaus, H. Bluhm, Optical layout and endstation concept for the enhanced Liquid interface spectroscopy and analysis (ELISA) beamline at BESSY-II, Synchrotron. Radiat. News 35 (2022) 67–72, https://doi.org/10.1080/08940886.2022.2082213.